

# Modelling for Improved Flood Forecasting in the Bow River Basin Using Prophet

A. A. Dash<sup>1\*</sup>, K. Castro<sup>1</sup>, and E. McBean<sup>1</sup>

<sup>1</sup> School of Engineering, University of Guelph, Guelph, Ontario N1G 2W1, Canada

Received 05 May 2024; revised 24 July 2024; accepted 23 September 2024; published online 02 December 2024

**ABSTRACT.** The catastrophic flood of the Bow River in 2013 had a significant impact on Calgary, Canada, and citizen's lives, showing the need for early warning systems and preparedness ahead-of-time. AI-based models that integrate climate and historical flow data, using the Prophet algorithm as applied in this research, demonstrate high accuracy in predictions for 15-, 10-, 5-day-ahead and 24-hour-ahead during extreme events in the Bow River, Banff. The predictions 5-day-ahead and 24-hour-ahead are 96.1% and 98.8% accurate, respectively, to the actual event on June 21<sup>st</sup>, 2013, as a particular case study. The Prophet algorithm shows significant benefits that maintain consistent nonlinear trends with daily, and weekly seasonality. This model also works with diverse components such as trends with high accuracy and greatly improves results using, for example, the GMDH algorithm. A comparison of evaluation metrics for the GMDH and Prophet models indicates that the GMDH model shows  $R^2$ , RMSE, and MAE values of 0.64, 46.8, and 6.70 respectively, with a disparity in accuracy and an absence of trend between the target and the dependent variables. The GMDH model performs well with a timestep of 17 h, but the accuracy significantly decreases with a timestep prediction of 120 h or 5-day-ahead, rendering the model's utility minimal. In contrast, the Prophet model features better prediction of time series data with higher evaluation metrics of  $R^2$ , RMSE, and MAE values of 0.97, 41.7, and 3.19, respectively.

**Keywords:** flood forecasting, bow river, prophet, flood risk, hydrological modeling, risk management

## 1. Introduction

Floods have been the largest damage hazard of worldwide natural disasters. Research showing natural disasters statistics around the world reported that floods that occurred between 2000 and 2019 have the highest number of events (3,254 events), and people affected (2.4 billion people) (UNISDR-CRED 2020). The year 2022 witnessed devastating floods in Pakistan that impacted 33 million individuals, resulting in 1,739 fatalities and a staggering economic loss of US\$ 15 billion. Floods also struck Bangladesh (7.2 million people affected), India (2,035 deaths, US\$ 4.2 billion of economic loss), and China (US\$ 5 billion of economic loss), etc. (EM-DAT, 2023).

Further, floods in Canada are the most common natural hazard according to the Canadian Disaster Database (Public Safety Canada, 2022). Figure 1 indicates that 336 flood disasters have occurred in Canada between the years 1900 and 2020, about twice as many as the next most common disaster, wildfire risk. Based on reports from the Alberta Treasury Board and Finance (2013) and Environment Canada (2014), the devastating floods that occurred in the Calgary area in June 2013 resulted in the destruction of ~ 4,000 businesses, 13,500 houses, forced about 100,000 people to evacuate, and resulted in five fatalities. The damages from this flood were at least ~ CAD\$6 billion, of

which ~ \$2 billion represented insured losses.

### 1.1. Literature Review

Since the frequency and severity of floods are expected to increase under climate change, especially in snowmelt-dominated areas, early warning systems are needed to support decision-making (Ebtejah and Bonakdari, 2022). Accurate and timely warning systems are key for mitigating the damages and loss of life from floods and hence, options to improve streamflow forecasting are of great importance (Xu et al., 2013) and can be broadly classified as process-driven and data-driven models (Wang, 2023).

Process-driven models are modeling approaches that are based on physical principles and typically involve a mathematical framework that considers the characteristics of the watershed and can play a crucial role in determining the streamflow process. (Wang, 2006). However, flood forecasts can also be both challenging to calibrate and computationally intensive (Leandro et al., 2009), often requiring lengthy running times (Lhomme et al., 2006) and input data may be unavailable (Chau, et al., 2005). Consequently, there is growing interest in cutting-edge data-driven models based on statistical relationships observed within hydrological variables such as streamflow (Samudrin et al., 2011).

AI-based and ML techniques, shown in Table 1, have been used by scholars for simulating different hydrological variables, including: rainfall, runoff, water level, river flow, and extreme floods. Instead of necessitating knowledge of specific assump-

\* Corresponding author. Tel.: 519-731-1368.

E-mail address: adash@uoguelph.ca (A. A. Dash).

tions to account for all hydro-geomorphological datasets associated with the watershed, these data-driven approaches “learn” from available data to detect relationships between them and to predict or recreate the outcome based on the recognized relationships (Hauswirth et al., 2023).

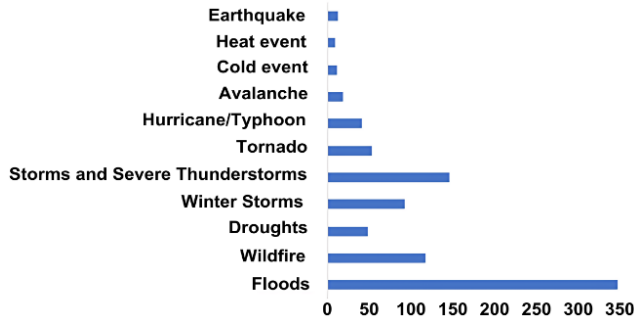


**Figure 1.** Natural Disaster Occurrences in Canada during 1900 to 2020 (Data were obtained from the Canadian Disaster Database).

In general, authors have found that deep machine learning techniques such as Artificial Neural Network (ANN), Long Short-Term Memory (LSTM), Support Vector Machine (SVM), achieve higher accuracies if compared to mathematical model techniques; however, some of them struggle with reconstructing trends and seasonality-based gaps to forecast stochastic hydrological processes such as daily precipitation, daily streamflow, or daily groundwater level. Other methods mentioned above, such as ANN and hybrid models, possess a complex architecture with several hidden layers and a few neurons in the input layer for non-expert stakeholders (Zhang et al., 2018).

A traditional machine learning model designed to handle time series with seasonal effects and trends, may be more suitable for flood forecasting tasks (Fronzi et al., 2024). For this reason, there is a crucial need for a fast, accurate, and tunable forecasting procedure that works best with time series with strong seasonal effects due to the oscillation of flows during the hydrologic years. Prophet is an open-source machine learning model specifically designed for time series forecasting, with a particular emphasis on capturing seasonality and trends (Taylor and Letham, 2018). Prophet is robust in automatically handling missing data and outliers, is flexible in incorporating domain knowledge, and can capture seasonality and holiday effects with simplicity.

## 1.2. Advantages and Disadvantages of Existing Machine Learning Models

Machine learning models, such as ANN, SVM, Random Forests (RFs), and Gradient Boosting Machines (GBMs), possess various advantages and disadvantages in flood forecasting and other time series prediction tasks. ANNs are highly effective at modeling complex, nonlinear relationships in data, which makes them suitable for hydrological forecasting (Mosavi et al., 2018); however, they require large datasets for training and are prone to overfitting, especially when the data is noisy or limited

(Kharroubi et al., 2016). SVMs excel in handling high-dimensional data and are robust against overfitting, making them useful for classification and regression tasks (Hamidouche et al., 2019). Nonetheless, SVMs can be computationally intensive and require careful parameter tuning, which can be time-consuming (Riad et al., 2004). RFs are known for their high accuracy and ability to handle large datasets with numerous features and are less prone to overfitting than individual decision trees (Dimopoulos et al., 1996) but the interpretability of RFs can be challenging, and they require substantial computational resources (Munji et al., 2013). GBMs, including XGBoost, offer robust performance and accuracy in regression and classification tasks, but they are prone to overfitting if not properly regularized and can be computationally expensive (Njoya et al., 2020). Overall, while these models provide powerful tools for forecasting, their complexity, computational demands, and potential for overfitting present significant challenges that must be managed to achieve optimal performance.

## 1.3. Shortcomings in Current Research

Despite the advances in ML models for flood forecasting, several shortcomings remain. Many models require extensive data preprocessing and are sensitive to missing values and outliers. The computational complexity of these models can be prohibitive, especially for real-time applications. Additionally, the interpretability of complex models such as ANNs and RFs poses challenges for their adoption in operational forecasting systems (Schulze et al., 2023).

## 1.4. Strengths of the Prophet Algorithm

The Prophet algorithm, developed by Taylor and Letham (2018), excels in time series forecasting due to its robustness to missing data and outliers, which minimizes the need for extensive data preprocessing. It is highly scalable, handling large datasets efficiently, making it suitable for real-time applications. Improving predictions using nonlinear regression models, particularly with outlier input data, is critical in achieving accurate streamflow forecasting (Hsieh, 2023). The model's additive framework, which decomposes time series data into trend and seasonality effects, enhances interpretability and simplifies the modeling process. Moreover, Prophet's user-friendliness and minimal requirement for parameter tuning make it accessible to users with varying levels of expertise. This flexibility allows for the incorporation of various seasonality, making it applicable to a wide range of forecasting problems, including hydro-meteorological applications.

## 1.5. Problems Addressed by Prophet

Prophet is particularly well-suited for hydrometeorological forecasting due to its ability to handle irregular time series data and integrate diverse data sources. Machine learning has shown potential in enhancing flood resilience, as demonstrated in its application to coastal areas like Morocco, which aligns with the use of the Prophet model for similar purposes (Satour et al., 2023). In this study, we leverage Prophet to forecast river

**Table 1.** Examples of Data-Driven Hydrological Forecasting Using Individual and Hybrid Machine Learning Models

Model Type	Previous Studies
Time Series Model	An autoregressive integrated moving average (ARIMA) model simulates the daily maximum streamflow from three-gauge stations, for example, the case of Cekerek Stream in Turkey, where Yurekli (2004) simulated daily maximum streamflow. Meanwhile, Noakes et al. (1985) conducted a study to assess the predictive capabilities of seasonal ARIMA, to predict monthly river flows across thirty rivers in North and South America, both autoregressive moving average (ARMA) and autoregressive (AR) models are utilized.
Artificial Neural Network (ANN)	Freiwan and Cigizoglu (2005) utilized an ANN approach in predicting the monthly precipitation in Jordan. Likewise, ANNs have been applied to predict the water levels in the unbounded aquifer located in the Lagoon of Venice, Italy., and the water levels in Lake Erie, Canada, with a 1-day lead time, using different ANN structures such as Multilayer Perceptron, M5P model tree, random forest, and k-nearest neighbors (Wang and Wang, 2020). It has been suggested by various studies that the use of a singular ANN model may not be sufficient in accurately predicting intricate issues, such as the processes of rainfall-runoff. For example, Tiwari and Adamowski (2017) combined the wavelet, bootstrap, and neural network (WBNN) models in a hybrid model to predict Calgary's daily urban water requirements.
Adaptive Neural-Based Fuzzy Inference System (ANFIS)	In the prediction of daily flow in the Karuvannur River Basin (India), the ANFIS model has demonstrated superior accuracy when compared to both the ANN and MNL models. The application of ANN and MNL models, along with ANFIS, have been instrumental in forecasting daily flow in the basin. (Anusree 2016). Similarly, Belvederesi et al. (2020) reported high accuracy using sequential ANFIS to predict flows along the Athabasca River in Alberta (Canada) with six-day forecast.
Support Vector Machine (SVM) and Least Squares Support Vector Machines (LSSVM)	SVMs, as described by Vapnik (1995), have found applications in various domains, such as hydrological and water resources planning (Wang et al., 2009; Asefa et al., 2006), for analyzing time series data. To address the cost aspect, Suykens and Vandewalle (1999) proposed a more affordable alternative called LSSVM, which is essentially a modified version of SVM. LSSVM offers a significant advantage over SVM as it tackles regression problems by employing a set of linear equations rather than quadratic programming.
Group Method of Data Handling (GMDH)	This model type was first developed by Ivakhnenko (1968). In their study, Samsudin et al. (2011) examined the application of a hybrid forecasting model to analyze monthly flow time series in various rivers of Malaysia. The researchers compared the performance of GMDH and LSSVM models for training and testing purposes. This model type was proposed to develop a time series prediction model within the Bow River in Calgary (Elkurdy et al., 2022). The $R^2$ , RMSE, and MAE values for the model's ability to forecast river discharge one day in advance were 0.64, 46.88, and 6.70, respectively.
Regression Models	Veiga et al. (2014) used historic daily river flow values in a multilinear regression model (MLR), from upstream stations (Banff and Seebe) to forecast the flows at Calgary, having an $R^2$ of 0.93. In the study conducted by Sehgal et al. (2014), a conventional MLR approach was employed to predict the daily flow in a delta region of the Mahanadi River basin in India. The resulting MLR model exhibited a relatively modest $R^2$ value of 0.671 when forecasting at a 2-day lead time., whereas the wavelet bootstrap-multiple linear regression (WBMLR) obtained $R^2 = 0.984$ .
Prophet	Prophet, an open-source time series forecasting library for business purposes, was developed by Taylor and Letham (2018) using Python and R. Only a very few studies have applied Prophet model for hydro-meteorological applications including Papacharalampous and Tyralis (2018), Papacharalampous et al. (2018a), two of which are pre-prints, not refereed papers.

flows in the Bow River Basin, incorporating both rainfall and snow data. Our approach aims to improve the accuracy and reliability of flood forecasts, addressing the limitations of existing ML models.

By integrating a comprehensive dataset and leveraging the strengths of the Prophet algorithm, this research contributes to the development of robust and efficient flood forecasting systems. The inclusion of diverse data sources, along with ontology-based approaches in AI, highlights the evolving role of advanced AI applications in hydrology (Baydaroğlu et al., 2023). This work not only enhances the predictive performance but also provides valuable insights for flood risk management and mitigation.

## 1.6. Objectives of This Study

As climate change is altering flood occurrence in Canada

(Buttle et al., 2016), there is a strong need to adapt flood forecasting systems to increase community resilience and reduce economic losses. In cold regions of Canada, challenges are that flood forecasting systems typically rely on rainfall-runoff models, which may not dedicate sufficient attention to all the cold region hydrological processes, and hydrometeorological observations are sparse or nonexistent. Machine learning methods only require historical values of the hydrological parameter from a basin and use a self-learning function to complete flood forecasting, preventing a complex modeling process.

Only a few studies have addressed different ML methods for predicting flooding events prior to its occurrence, in Canadian river basins (e.g., Veiga et al., 2015; Walton et al., 2019; Belvederesi et al., 2020; Elkurdy et al., 2022; Ebtejah and Bonakdari, 2022; de Oliveira et al., 2023). Regarding Prophet, researchers have tested it for groundwater level estimation

(Aguilera et al., 2019; Zarinmehr et al., 2022), precipitation prediction (Galdelli et al., 2023) and forecasting of monthly streamflow (Papacharalampous and Tyrallis, 2018). In these studies, Prophet performed well compared with other univariate time series methods such as ARIMA (Aguilera et al., 2019). However, no research has been identified wherein Prophet has been successfully utilized for flood forecasting, specifically for predicting flows over a series of timeframes that would be useful in-situ.

This paper describes the development of Prophet algorithm for forecasting extreme events in a cold weather region, Bow River in Alberta, Canada. To assess the utility of a flood forecasting model with sufficient lead time to conduct emergency evacuation plans, the Prophet model is described for estimating different lead-times, ranging from 15- to 1-day-ahead of flooding events. For this approach, Prophet is employed using historical data to anticipate future events. For example, to forecast the events of 21<sup>st</sup> June 2013, datasets as far ahead as 11<sup>th</sup> June 2013 were employed using Prophet, to predict future events based on information available on 11<sup>th</sup> June 2013 to assess its accuracy. The predictions are described for 15- and 10-day-ahead, and 12-hour-ahead, as described in the next section.

## 2. Methodology

### 2.1. Study Area and Datasets

The basin of Bow River at Banff follows the main valley of the Bow River through mountainous terrain with glaciers and icefields. The ecosystems presented in the surroundings of Banff National Park are montane (~ 3%), subalpine (~ 53%), and alpine (~ 27%). Forests cover 44% of Banff National Park, primarily in valley bottoms and lower mountain hillslopes (Van Wagner et al., 2006). The upper Bow River receives an annual precipitation of 500 to 700 mm, with half falling as snow, while Calgary receives 412 mm of annual precipitation, with 78% of in the form of rain. (Bow River Basin Council, 2010). Figure 2 presents the map of the study area, with the selected station. The flow of the river is greatly impacted by the climate conditions prevalent in southern Alberta, which are marked by prolonged, chilly winters and brief, hot summers. The Banff area has a cold temperate climate, with an average annual temperature of -0.4 °C. The dominant hydrological event is melting of the winter snowpack combined with the onset of spring rains, leading to peak river discharges from May to June.

The Bow River at Banff hydrometric station has functioned since 1909, and data from this site have been used in studies of mountain hydrology and flooding (Pomeroy et al., 2016; Rood et al., 2016; Whitfield and Pomeroy, 2016). Having lengthy records is a critical component for flood forecasting and disaster warning. The present work applied precipitation records (rainfall, snowfall), river flows and temperature time series from May 5<sup>th</sup>, 1909, to June 21<sup>st</sup>, 2013, recorded daily and collected from Environment Canada website for the Banff station in Alberta. In addition, mean daily streamflow data, compiled by Alberta Environment and Parks for the period 1910 ~ 2010 at Banff station, were also integrated into the model.

Selections of these locations were based on the dependability and availability of the data.

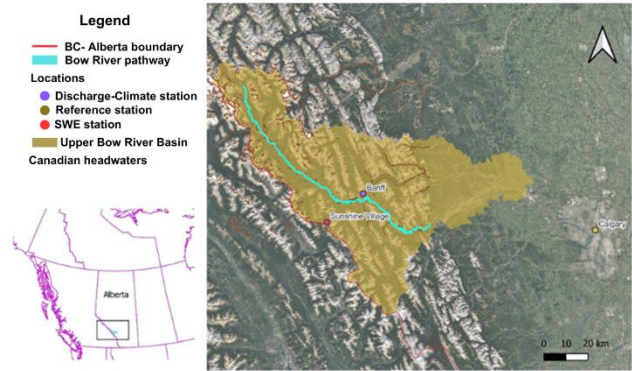


**Figure 2.** Location of the Bow River Basin and monitoring stations. The figure spans from the starting point of the Bow River to a location immediately upstream of Calgary.

### 2.2. Proposed Model: Prophet Algorithm

The Prophet model is an additive model which adjusts to achieve smooth curves from complex time series patterns and is classified with periodic components (Taylor and Letham, 2018). The decomposition of time series models involves three primary components: trend, seasonality, and holidays. The components are represented in Equation (1) as:

$$y(t) = g(t) + s(t) + h(t) + \epsilon_t \quad (1)$$

where the trend component of the time series, which captures non-periodic fluctuations, is denoted by the function  $g(t)$ . However, the function  $s(t)$  takes into consideration regular fluctuations such as seasonality, while the function  $h(t)$  captures the impact of holidays that may occur on unpredictable schedules lasting for one or more days. The error term  $\epsilon_t$  is responsible for capturing any unexplained idiosyncratic changes that are not considered by the model. In the flood prediction model, time can be used as a regressor, along with multiple linear and non-linear functions of time as components. The modeling of seasonality as an additive component follows a similar approach to that achieved through exponential smoothing. (Machiwal and Jha, 2012; Zarinmehr et al., 2022).

The Generalized Additive Models (GAMs) formulation offers the benefit of easy decomposition and flexibility to incorporate new components as required. This means that it can easily accommodate new sources of seasonality, such as the influence of climate change, when they are identified. GAMs also easily fit the data using back-fitting, in a way that allows for interactive manipulation of the model parameter such as seasonality (yearly, weekly or daily), growth trend (linear or logistic), and regularization (ridge regression). Essentially, the Prophet approach to forecasting is being framed as a curve-fitting task, and hence is distinct from time series models as Prophet does not account for the temporal dependence structure

inherent in the data, such as present in Elkurdy et al. (2022).

### 2.3. How the Algorithm Calculates the Trend Days/Weeks Ahead

Two trend models cover the forecasting applications in the Prophet model: a saturating growth model, and a piecewise linear model.

The primary element of the data-generating process in a Prophet flow forecasting model involves evaluating the extent to which the flow has expanded and the projected growth. Utilization of Prophet for flow modeling often resembles the growth of populations in natural ecosystems, where there is nonlinear growth that reaches so-called a “saturation” point at a carrying capacity. For example, the carrying capacity for the Bow River in Banff region might be the temperature extremes, snowpack, and precipitation in that area.

This type of growth is commonly depicted by the logistic growth model, which is typically expressed in its simplest form as (2):

$$g(t) = \frac{c}{1 + \exp(-k(t - m))} \quad (2)$$

with  $c$  as the carrying capacity/flow in the Bow River,  $k$  is the growth rate, and  $m$  is an offset parameter.

The carrying capacity  $g(t)$  is not constant, as  $g(t)$  is based on the temperature, snowmelt or rainfall increase, as does a growth ceiling. Hence, the constant capacity  $c$  is being substituted with a capacity  $c(t)$  that varies with time. Additionally, the growth rate “ $k$ ” is not consistent, and any extreme climate event can significantly impact the flow rate in the Bow region. As a result, the model includes trend rates to accurately represent historical data.

The growth model has been modified to include specific points where the growth rate or flow can change. Assume there are  $s$  change points at times  $s_j$ , where  $j = 1, 2, 3, \dots, s$ . A set of rate adjustments  $\delta \in \mathbb{R}^s$  defined, with  $\delta_j$  representing the rate change that occurs at time  $s_j$ . The rate at any given time  $t$  is calculated as the base rate  $k$ , plus the sum of all adjustments up to that point:

$$k + \sum_{j:t > s_j} \delta_j \quad (3)$$

This is represented by defining a vector  $a(t) \in \{0, 1\}^s$  such that:

$$a_j(t) = \begin{cases} 1, & \text{if } t \geq s_j \\ 0, & \text{otherwise} \end{cases} \quad (4)$$

The expression  $k + a(t)^T \delta$  represents the rate at time  $t$ . To link the endpoints of the segments, it is necessary to modify the offset parameter “ $m$ ” in conjunction with the rate “ $k$ ”. The computation for determining the accuracy adjustment at change point  $j$  is as follows:

$$\gamma_j = \left( s_j - m - \sum_{l < j} \gamma_l \right) \left( 1 - \frac{k + \sum_{l < j} \delta_l}{k + \sum_{l < j} \delta_l} \right) \quad (5)$$

The piecewise logistic growth model is then:

$$g(t) = \frac{c(t)}{1 + \exp(-k + a(t)^T \delta) \left( t - (m + a(t)^T \gamma) \right)} \quad (6)$$

The anticipated capacities of the Bow River at any given moment, also known as  $c(t)$ , are a crucial set of parameters in this application.

The trend will have a constant rate when the model is extrapolated beyond the forecast timeframe, to make a forecast for “ $x$ ” days in the future. The level of uncertainty in the forecast trend has been assessed by extending the generative model into the future. The trend’s generative model comprises  $S$  change points across a history of  $T$  points. Each point experiences a rate change  $\delta_j$ , which follows a Laplace distribution with parameters  $(0, \zeta)$ . To forecast future rate fluctuations, the past is replicated by replacing  $\zeta$  with a variance calculated from the existing data. A hierarchical approach prior on  $\zeta$  can be utilized within a comprehensive Bayesian framework to attain its posterior probability. An alternative approach involves the utilization of the maximum likelihood estimate for the rate scale parameter, denoted by:

$$\lambda = \frac{1}{s} \sum_{j=1}^s |\delta_j| \quad (7)$$

The future change points are randomly selected to ensure that the frequency of change points aligns with the historical average:

$$\forall j > T, \begin{cases} \delta_j = 0 \text{ w.p. } \frac{T-3}{T}, & \text{if } t \geq s_j \\ \delta_j \sim \text{laplace}(0, \lambda) \text{ w.p. } \frac{3}{T} \end{cases} \quad (8)$$

The level of uncertainty in the forecast trend is measured by assuming that the future will demonstrate a similar average frequency and magnitude of rate changes as observed in the historical data up until the point of forecasting. Once the data has been used to infer  $\lambda$ , the generative model aims to replicate potential future patterns and utilize these patterns to calculate intervals of uncertainty. It is assumed that the frequency and magnitude of the trend will persist in the same manner as observed in the past, if the history is robust, containing alternative (earlier) scenarios; while it cannot be guaranteed that the uncertainty intervals will be perfectly accurate, they do provide valuable insight into the degree of uncertainty present, particularly regarding overfitting. As the value of  $\zeta$  increases, the model becomes more adaptable to the historical data, resulting in a reduction of training error. However, when anticipated in the future, this flexibility will lead to significant uncertainty intervals.

Overall, the Prophet model is mostly relevant in events where historical data are measured as a dependable indicator for future trends, but there is also identification that differences and uncertainties occur. It provides an organized way to combine this historical data into prediction, while explicitly incorporating uncertainty.

## 2.4. Performance Indicators

The comparative performance of the model has been assessed in terms of MAE, MAPE, RMSE error, and the  $R^2$ .

### 2.4.1. R-Squared (Coefficient of Determination)

R-squared (see Equation (9)) measures the proportion of variance in the dependent variable ( $y_{true}$ ) that is explained by the independent variables ( $y_{pred}$ ). It ranges from 0 to 1, with 1 indicating a perfect fit:

$$R^2 = \frac{\sum (y_i - \bar{y})^2}{\sum (y_i - y_i)^2} \quad (9)$$

where  $\sum$  represents the sum of squared differences between the predicted and actual values and  $y_{mean}$  is the mean of the actual values. The  $R^2$  values for the three extreme events of the year 1929, 2012, and 2013 are explained in further detail (Section 3.5, Figure 8).

The  $R^2$  value serves as a statistical indicator that assesses the alignment between the Prophet model and the observed data. Essentially, the Prophet model quantifies the extent to which the model's  $p$  predictions capture the variations in the stream flow data. This measure ranges from 0 to 1, with higher values indicating a more robust correspondence between the predicted and actual values:

$$R^2 = 1 - \frac{RSS}{TSS} \quad (10)$$

where  $TSS$  = sum of the squared differences between each observed value and the mean of the observed values, and  $RSS$  = sum of the squared differences between each observed value and the corresponding predicted value by the model.  $R^2$  calculates the proportion of the total variance in the dependent variable (stream flow) that is captured by the model.

The  $R^2$  values for each individual year offer a comparative assessment of the model's ability to predict occurrence over various time segments and thus enable it to be evaluated as efficient at matching forecasts with observed stream flow data in any given year. Each  $R^2$  value indicates how well the Prophet model's predictions are at aligning with observed streamflow data for this period, representing its goodness-of-fit to that particular year.

### 2.4.2. RMSE (Root Mean Squared Error)

RMSE is calculated by taking the square root of the aver-

age of the squared differences between the predicted values and the actual values (see Equation (11)). The RMSE ranges from 0 to  $\infty$ , and lower values indicate fewer errors between the model predictions and the actual values:

$$RMSE = \sqrt{\frac{\sum_{i=1}^n (y_i - \hat{y}_i)^2}{n}} \quad (11)$$

Figure 3 shows the Root Mean Square Error for "Normal" and "Extreme Event". The lower the RMSE values, the higher the prediction accuracy. Figure 3 shows lower RMSE values for 24 h and 5-head-day predictions in comparison to 10- and 15-head-day streamflow predictions indicating a better performance accuracy.

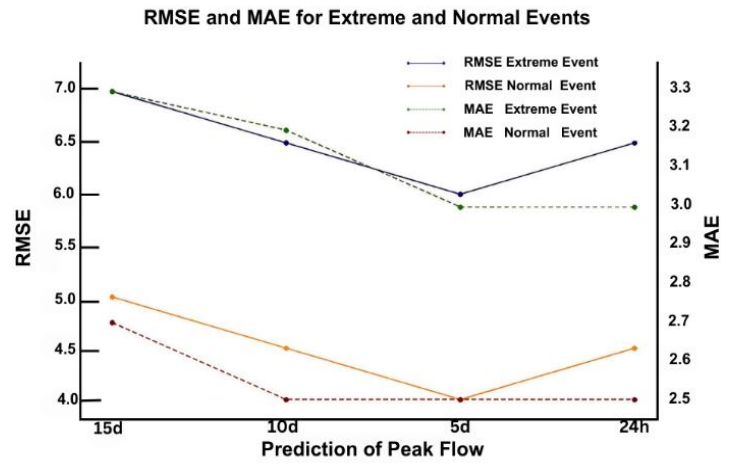


Figure 3. Measures for forecast accuracy.

### 2.4.3. MAE (Mean Absolute Error)

MAE is the difference between the actual and predicted values (see Equation (12)). The values range from 0 to  $\infty$ , and lower values indicate less error in model predictions.

$$MAE = \frac{1}{n} \sum_{i=1}^n |y_i - \hat{y}_i| \quad (12)$$

Figure 3 shows the MAE for "Normal" and "Extreme" event (such as in 2013), respectively. The lower the MAE the better is the prediction accuracy. Figure 3 shows lower MAE value for 24 h, 5-head-day prediction in comparison to 10- and 15-head-day stream flow prediction. Lower MAE value in 24 h, 5-head-day prediction indicates lower variation of streamflow prediction from the actual values depicting the utility of the Prophet model.

### 2.4.4. MAPE (Mean Absolute Percent Error)

A slight modification of MAE in which the difference between predicted and observed examples is divided by the true value predictions and can constrain the error to a smaller range:

$$MAPE = \frac{1}{n} \sum_{i=1}^n \left| \frac{y_i - \hat{y}_i}{y_i} \right| \quad (13)$$

The MAPE for the extreme event of 2013 has been calculated to be 4.89%, indicating that the prediction is acceptably accurate.

### 3. Results and Discussion

The time series used in this study is the daily flow of the Bow River at Banff Basin. The time series utilized encompasses the period from May 5<sup>th</sup>, 1909, to June 21<sup>st</sup>, 2013, and is divided into training and test datasets. It is noted that the dataset available for this research continues up to October 31<sup>st</sup>, 2022; however, for the prediction analyses for 2013 (the catastrophic flood event of that year) data utilized were restricted only to data prior to the date of forecasting. For example, for 5-day-ahead prediction for June 21<sup>st</sup>, 2013, the training data consists of historical information up to 16<sup>th</sup> June 2013.

#### 3.1. Prediction Accuracy for 1-Day Ahead Prediction

Figure 4 shows 1-day-ahead prediction for the 21<sup>st</sup>, June 2013 event and the temporal variations of the actual flow of Bow River. The discrepancy between the forecast value and the actual flow is the timeframe ahead where the prediction is 24-hour-ahead. The June 21<sup>st</sup>, 2013 is considered an extreme event in this research as this was the time of one of the most extreme, destructive flood events that have occurred in Canada. The comparative difference between the observed and 1-day-ahead prediction considering the extreme event time series, or absolute error, shows that the Bow River flow peaked in June at 450 m<sup>3</sup>/s. The 1-day-ahead prediction in the Banff station showed an  $R^2$  of 0.98, indicating the excellent efficacy of the model.

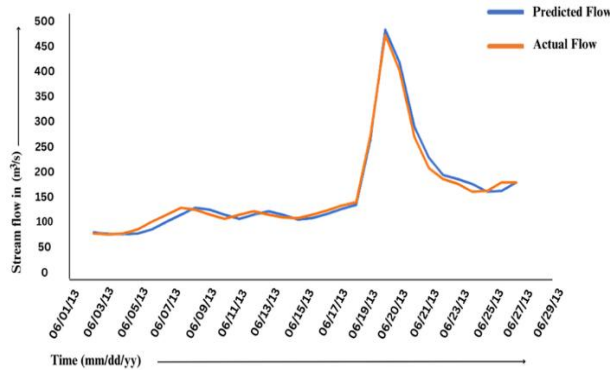


**Figure 4.** Line graph of prediction accuracy, of Prophet algorithm, using flow time series data of the Bow River at Banff, station for 1-day-ahead prediction and the measured flows.

#### 3.2. Time Series Classification

This study involves developing predictions for extreme event conditions of time series. Extreme event conditions are rare occurrences that have a significant impact on the flow, and

hence, the flood event in the Bow River at Banff station which occurred on June 21<sup>st</sup>, 2013.

#### 3.3. Prophet Model (15-, 10-, 5-Day and 24-Hour-Ahead Predictions)

Figures 5 show the assembly of 15-day-ahead, and 5-day-ahead predictions of flow for the Bow River at Banff station for 2013 extreme event. The predictions for the different timesteps are:

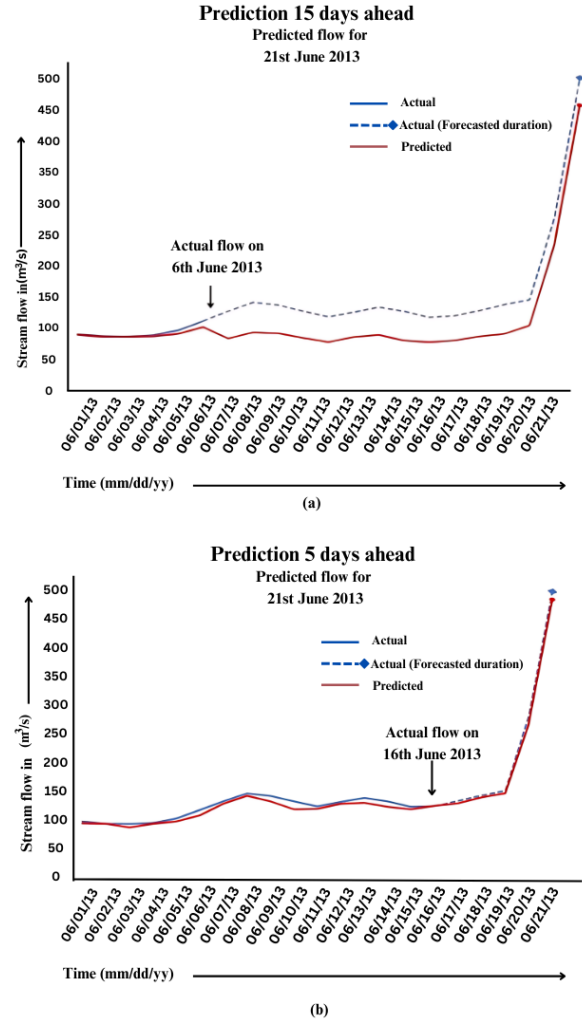


**Figure 5.** Streamflow predictions for the bow river at banff station during the 2013 extreme event: a comparative analysis across varied forecast horizons using the prophet model (a) prediction 15-day-ahead, (b) prediction 5-day-ahead.

**(a) 15- and 10-day-ahead prediction.** The longer the forecasting horizon, the lower is the accuracy of the Prophet model. The 15- and 10-day-ahead prediction for the 2013 extreme event is 91.50 and 91.80% accuracy to the actual flow. As the forecasting horizon is increased (forecasting further into the future), the instability of predictions increases (less accuracy).

**(b) 5-day-ahead prediction.** Prophet was also used to make

predictions by using a 5-day-ahead forecast horizon. The “time stamp” column also known as “ds” is set for the 5-day-ahead prediction and then the model initiates predictions for each of the specific dates. The 5-day-ahead prediction for the 2013 extreme event is 96.10% accurate to the actual flow on June 21<sup>st</sup>, 2013.

**(c) 24-hour-ahead prediction.** The 24 h prediction requires the historical data of the past to forecast the next 24 h. The datasets used in this study were for the year 1909 and are in time series format with relative timestep flow values. The 24 h prediction for the flood (i.e., 2013 extreme event) is 98.80% accurate to the actual flow.

As apparent, the predictions continue to improve for the June 21<sup>st</sup>, 2013, event. The predictions 5-day-ahead and 24-hour-ahead are 96.10 and 98.80% accurate, respectively, to the actual event on June 21<sup>st</sup>, 2013.

### 3.4. Prophet Model Predictions for Peak Stream Flows

The model prediction accuracy 5-day-ahead increases in a linear trend with the increase of the historical flow data. To demonstrate this aspect, the prediction accuracy for an earlier event (recall that the 1929 year had only 20 years of historical data from which to learn); Figure 6 shows the prediction accuracy for the year 1929, the model achieves an accuracy of 87.50% to the actual flow (i.e. lesser accuracy because there were fewer data available for the model to “learn” from available data). As further demonstration, the Prophet model was used to predict the 5-day-ahead peak flow in 2012 (using only the data available up to the time of prediction), the accuracy increased to 93.50%, indicating improved model’s predictive ability with the increase of available, historical data. In 2013, the accuracy further increased to 96.10% to the actual flow. Clearly, the model’s ability to provide accurate forecasts increases with an increase of historical data.

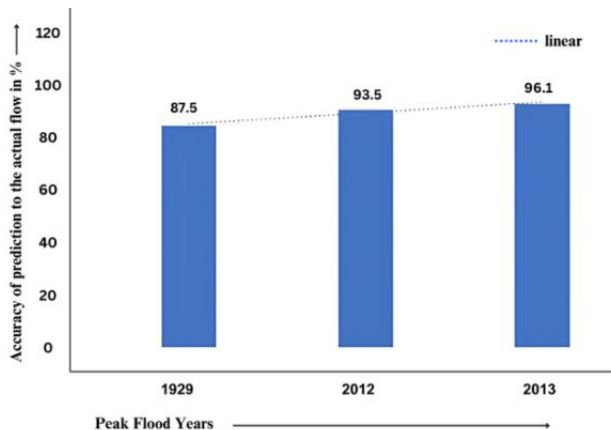


**Figure 6.** Prophet model prediction accuracy in percentage for several peak flows predicted 5 days ahead.

The 5-day-ahead Prophet model prediction for 1929 and 2012 extreme events is shown in Figure 7. The predictions utilize the past trends, seasonal influences, and the fluctuations in stream flow. By providing increased availability of data pre-

ceding historical events, Prophet makes predictions for extreme events such as 1929, 2012, and 2013 flood across the Bow River at Banff station.

### 3.5. Evaluation Metric of the Prophet Model

Figure 8 shows  $R^2$  values of 0.9830, 0.9810 and 0.9700 for the three extreme events of the year for 1929, 2012 and 2013. The  $R^2$  value of the year 2013 is lower than 1929 due to the change of underlying patterns, trends, and seasonal conditions of stream flows over the given time period. Other factors such as climate change, environmental variations, or human interventions (e.g., dam constructions, land use changes) could have influenced stream flow patterns over the years. Lower  $R^2$  values, is due to unexpected changes or events occurring in 2013 that differ considerably from  $R^2$  value is comparatively lower than the year 1929, but the model’s prediction accuracy is higher (as shown in Figure 8).

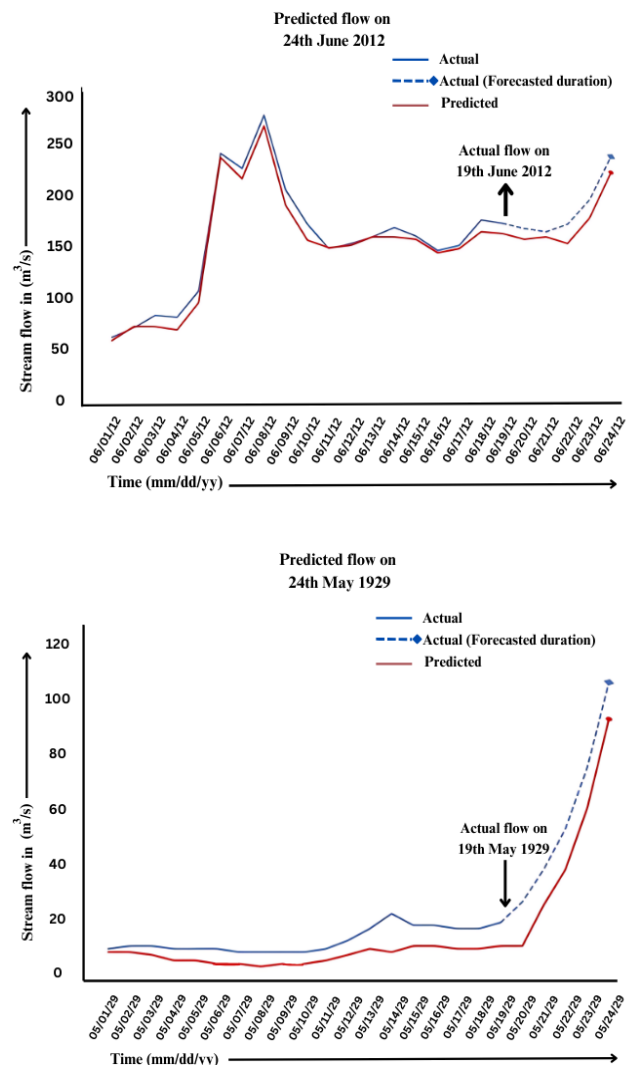


**Figure 7.** Stream flow predictions (5-day-ahead) for the Bow River at Banff station during the 1929 and 2012 extreme event.

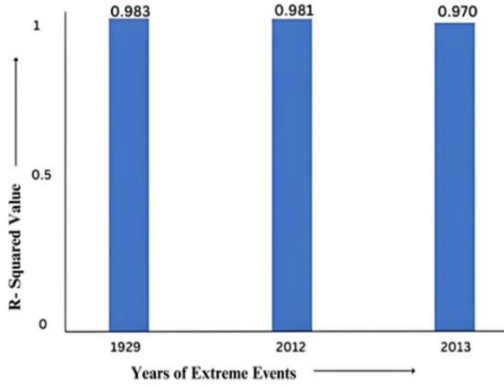


**Figure 8.** Graph showing  $R^2$  value of 1929, 2012 and 2013 ex- treme flood events.

The interpretation of  $R^2$  is crucial when using it as an evaluation metric. A value close to 1 indicates a strong fit, indicating that the model closely replicates the observed data trends. Within the Prophet framework, this metric is valuable for comparing different model iterations or configurations. Models with higher  $R^2$  values are typically preferred as they have a better ability to capture the variability in stream flow, which can result in more precise predictions.

### 3.6. Evaluation of Two Different Time Series Forecasting Models for Stream Flow Prediction

This study involves “degree” to which, for example, day-ahead forecasting of stream flow can be done so that necessary action can be undertaken in the events of flows at a level that will ultimately cause flooding. Issues such as these have been investigated (e.g., Elkurdy et al., (2022)) for the Bow River where they reported the use of Group Method of Data Handling (GMDH) model for advanced recognition of the flooding of the Bow River in Alberta, Canada. The GMDH method performed well for stream flow predictions with 3-hour-ahead time and has shown an  $R^2$  value of 0.90 with 17-hour-ahead prediction. However, when the timestep of the model is increased from 17 to 24 h, the model quickly loses its robustness and accuracy. A comparison of evaluation metrics for the GMDH and the Prophet model is indicated in Table 2. The GMDH model shows  $R^2$ , RMSE, and MAE values of 0.64, 46.80 and 6.70, respectively, with a disparity in accuracy and delineating the absence of trend between the target and the dependent variables. The GMDH model performs well with a timestep of 17 h, but the accuracy significantly decreases with a timestep prediction of 120 h or 5-day-ahead such that the utility of the model becomes minimal.

As evident from Table 2, the Prophet model features a better prediction of time series data with higher evaluation metrics of  $R^2$ , RMSE, and MAE values of 0.97, 41.70, and 3.19 as compared to that of the GMDH model. The Prophet model shows a higher accuracy of prediction with 120-hour-ahead or 5-day-ahead of time as compared to the GMDH model which has 3 h timesteps of predictability. A comparison with the GMDH model is used to demonstrate the comparability to the Prophet model

as shown in Table 3.

**Table 2.** Evaluation Metrics for GMDH and Prophet Model at 5 Days Ahead Prediction

Evaluation Metrics	GMDH Model	Prophet Model
$R^2$	0.64	0.97
RMSE	46.80	41.70
MAE	6.70	3.19

Moreover, aside from its ability to make long-term forecasts, the Prophet algorithm offers significant benefits as an additive model that maintains consistent nonlinear trends with daily, weekly, and yearly seasonality. The Prophet also works with diverse components such as trend. As a result, the model shows higher accuracy and can work with missing data (i.e., datasets in which some data points are missing). Elkurdy et al. (2022) presented GMDH model which does not have the ability to work with the missing data. The Prophet model also performs well with the outliers and addresses the collinearity between the input variables. In the case of an extreme event such as of June 21<sup>st</sup>, 2013 the Prophet model has shown an  $R^2$  value of 0.97 in 5-day-ahead prediction. The higher  $R^2$  value indicates the better performance of the model and its ability to make correct predictions. The Prophet model with higher accuracy can follow the trends and historical patterns of the data and can make predictions close to the actual values.

### 3.7. Comprehensive Data Integration

Our study leverages an extensive dataset spanning over a century, from May 5<sup>th</sup>, 1909, to June 21<sup>st</sup>, 2013, collected from the Bow River at Banff Basin, Calgary. This dataset includes daily records of river flow, precipitation (both rainfall and snowfall), and temperature, offering a comprehensive view of the hydrological patterns in the region. The inclusion of snow data is particularly significant, as snowmelt contributes substantially to river flow in cold regions. This detailed and diverse dataset allows the model to capture a wide range of hydrological variability, improving its predictive performance. The use of such a comprehensive dataset ensures that the model is trained on a variety of scenarios, making it more robust and reliable in predicting future events. This extensive dataset enhances the model’s ability to identify and learn from historical trends, seasonal variations, and extreme events, which are crucial for accurate long-term forecasting. Recent studies highlight the importance of integrating diverse hydrological data to improve forecasting models, reinforcing the value of our comprehensive approach (Slater et al., 2023).

### 3.8. Practical Implications

The practical implications of our study are profound, especially in the context of flood risk management and early warning systems. Accurate and timely flood forecasts are critical for mitigating the impacts of flooding, including loss of life, property damage, and economic disruption. The Prophet model’s ability to provide reliable forecasts with sufficient lead time of-

**Table 3.** Comparison of Elkurdy et al. (Elkurdy et al., 2022)'s GMDH Model and Prophet Model

Comparison Criteria	GMDH Model	Prophet Model
Evaluation Metrics ( $R^2$ , RMSE, MAE)	The evaluation metrics of the model for 24h-day-ahead is $R^2$ , RMSE and MAE are 0.64, 46.80 and 6.70 respectively.	The evaluation metrics of the model for 24h-day-ahead is $R^2$ , RMSE and MAE is 0.97, 41.70 and 3.19 respectively.
Trend and Noise	Disparity with accuracy, and mostly noisy, without featuring any trend between the factors and target variables.	The time series data are constructed using an additive model, which incorporates non-linear trends and accounts for yearly, weekly, and daily seasonality. Prophet implements an additive regression model with elements such as a piecewise linear model, where the model automatically identifies change points in the data and indicates any change in the trend.
Inclusion of Important Regressors	Absence of inclusion of important regressors such as snowpack, precipitation etc.	Performs efficiently with time series exhibiting prominent seasonal patterns and multiple seasons of past data. (Including temperature, precipitation, and snowpack data)
Overfitting	The quality of the prediction result is affected due to overfitting.	The model doesn't require performing data preprocessing and works with missing data along with several outliers.
Prediction of Extreme Events	The model was able to predict the dailyflow rate accurately but has a limitation in predicting the implications of severe and unpredictable conditions.	The model showed a greater accuracy than GMDH model of prediction for extreme events.
Short-term Prediction Accuracy	The model has been able to predict 17 h ahead effectively but the accuracy declined with subsequent hours.	The model was able to predict on a weekly, monthly and quarterly basis with difference in accuracy.
Handling Extreme Events (e.g., 2013)	The daily model suffers from poor prediction in case of extreme events such as for 2013 event.	The model predicted well for the extreme event such as 21 <sup>st</sup> June 2013 with a $R^2$ value of 0.97.
Lead Time for High-Flow Events	The hourly prediction model predicts high flows 3h advance in time, thus allowing only minimal time intervals for the community to take the necessary steps to minimize flooding impacts.	The model has been able to predict with greater accuracy, 3 to 4 days ahead, thereby allowing necessary steps to be taken to warn of imminent flooding.
Overall Prediction Horizon	The model shows greater accuracy with extreme low time intervals such as 3 h.	The model can predict accurately 5 days or (120 h) ahead.

fers several key benefits. Enhanced early warning systems can alert residents and authorities in advance, enabling timely evacuations and preparations to minimize the impact of flooding. Improved emergency response planning is another significant benefit, as reliable forecasts allow emergency response teams to better allocate resources and plan interventions. This proactive approach enhances the efficiency and effectiveness of emergency response efforts, reducing potential losses. Additionally, the model's long-term forecasting capabilities provide valuable insights for infrastructure management and maintenance. Authorities can use these forecasts to plan and implement flood control measures, such as reservoir management, levee construction, and drainage improvements. By integrating accurate flood forecasts into community planning and risk management strategies, communities can enhance their resilience to flooding events, aligning with recent studies on disaster risk reduction and community resilience.

### 3.9. Limitations and Future Work

While our study demonstrates significant advancements in flood forecasting using the Prophet model, several limitations warrant further investigation. The model's accuracy depends heavily on the availability and quality of historical data. Signif-

icant changes in underlying conditions, such as climate change, land use changes, or human interventions, may impact the model's predictive performance. Future research should explore methods to integrate external factors and covariates that influence river flow dynamics, such as real-time meteorological data, land use data, and climate change projections. The Prophet model may also struggle with datasets that have irregularly spaced time intervals or extensive missing data points. Future work should investigate approaches to improve the model's performance in handling irregular time series data, such as data imputation techniques or hybrid models that combine Prophet with other machine learning methods. The Prophet model is designed to provide accurate forecasts for relatively short to medium-term horizons such as three to four weeks ahead. Forecasting further into the future, especially beyond a year or two, might lead to greatly deterioration/diminished predictions due to the model's reliance on historical patterns and seasonality.

Furthermore, validating the model's generalizability and robustness by applying it to other river basins and hydrological contexts is essential. Future research should involve testing the model in diverse geographical and climatic settings to assess its applicability and performance across different regions, as highlighted in recent hydrological modeling studies.

#### 4. Conclusion

Prophet modeling demonstrates timely accuracy in flood prediction, making it an invaluable tool for early warning systems aimed at reducing the disastrous impacts of floods. Its ability to accurately imitate underlying trend patterns results in highly reliable predictions. By integrating historical data with current meteorological conditions, Prophet offers excellent potential as an early warning system, facilitating flood damage reduction.

In this study of stream flow predictions for 15-, 10-, 5-day, and 24-hour-ahead forecasts during an extreme event in the Bow River, Banff, the Prophet model showed higher accuracy compared to the GMDH model. This accuracy is crucial for allowing warning systems to effectively disseminate information about upcoming floods, thereby mitigating the damage caused by such events. The results highlight the utility of artificial intelligence in predicting floods for significant events over the last several decades.

Moreover, the modeling results illustrate how the accuracy of predictions improves with the Prophet model as the available database for model development increases. This enhancement is particularly significant for regions with extensive historical data, enabling more precise and timely flood forecasts. The ability of Prophet to handle large datasets efficiently and its robustness to missing data and outliers further underscore its suitability for real-time flood forecasting applications.

The extended lead time provided by the Prophet model, which accurately forecasts up to 5-day-ahead, is a substantial improvement over the 17-hour lead time of the GMDH model. This extended forecasting capability allows for more proactive measures, better resource allocation, and enhanced community preparedness. As a result, communities can respond more effectively to impending flood events, reducing the socio-economic impacts and enhancing overall resilience.

In the future, expanding the use of the Prophet model to incorporate real-time meteorological data, climate change projections, and land-use changes will further improve its accuracy and applicability. Additionally, testing the model in diverse geographical regions and integrating external factors, such as glacier melt and hydrological variability, could broaden its use for flood risk management in different contexts. The model's potential applications extend beyond flood forecasting to other time series prediction tasks in hydrology, offering a pathway to more resilient and informed decision-making in water resource management.

Therefore, the Prophet model's superior accuracy, scalability, and user-friendliness make it a highly effective tool for flood forecasting. Its integration into early warning systems provides the opportunity to significantly enhance flood risk management, offering a reliable and efficient means to safeguard communities against the adverse effects of flooding. The study's findings underscore the importance of using advanced machine learning models like Prophet to improve the predictability and management of flood risks.

**Acknowledgments.** Funding from NSERC (RGPIN-2023-03391),

Skills for Communicating Change in Agri-food Scholarship (E/I6084), and Nora Cebotarev Memorial Scholarship is gratefully acknowledged.

#### References

- Aguilera, H., Guardiola-Albert, C., Naranjo-Fernández, N. and Kohfahl, C. (2019). Towards flexible groundwater-level prediction for adaptive water management: Using Facebook's Prophet forecasting approach. *Hydrological Sciences Journal*, 64(6), 1504-1518. <https://doi.org/10.1080/02626667.2019.1651933>
- Alberta Treasury Board and Finance (2013). *Budget 2013-2014 first quarter fiscal update and economic statement*. Alberta Treasury Board and Finance.
- Anusree, K. and Varghese, K. (2016). Streamflow prediction of Karuvannur River Basin using ANFIS, ANN and MNL models. *Procedia Technology*, 24, 101-108. <https://doi.org/10.1016/j.protcy.2016.05.015>
- Asefa, T., Kemblowski, M., McKee, M. and Khalil, A. (2006). Multi-time scale stream flow prediction: The support vector machines approach. *Journal of Hydrology*, 318, 7-16. <https://doi.org/10.1016/j.jhydrol.2005.06.001>
- Baydaroglu, Ö., Yeşilköy, S., Sermet, Y. and Demir, I. (2023). A Comprehensive review of ontologies in the hydrology towards guiding next generation artificial intelligence applications. *Journal of Environmental Informatics*, 42(2), 90-107. <https://doi.org/10.3808/jei.202300500>
- Belvederesi, C., Dominic, J.A., Hassan, Q.K., Gupta, A. and Achari, G. (2020). Predicting river flow using an AI-Based sequential adaptive neuro-fuzzy inference system. *Water*, 12(6), 1622. <https://doi.org/10.3390/w12061622>
- Bow River Council (2010). *Bow River Basin State of the Watershed Summary*. Bow River Council.
- Chau, K.W., Wu, C.L. and Li, Y.S. (2005). Comparison of several flood forecasting models in Yangtze River. *Journal of Hydrologic Engineering*, 10(6), 485. [https://doi.org/10.1061/\(ASCE\)1084-0699\(2005\)10:6\(485\)](https://doi.org/10.1061/(ASCE)1084-0699(2005)10:6(485))
- de Oliveira, A.K.B., Carneiro Alves, L.M., Carvalho, C.L., Haddad, A. N., de Magalhães, P.C. and Miguez, M. G. (2023). A framework for assessing flood risk responses of a densely urbanized watershed, to support urban planning decisions. *Sustainable and Resilient Infrastructure*, 8(4), 400-418. <https://doi.org/10.1080/23789689.2023.2175139>
- Dimopoulos, I., Lek, S. and Lauga, J. (1996). Modélisation de la relation pluie-débit par les réseaux connexionnistes et le filtre de Kalman. *Hydrological Sciences Journal*, 41(2), 179-193. <https://doi.org/10.1080/02626669609491491>
- Ebtehaj, I. and Bonakdari, H. (2022). Early detection of river flooding using machine learning for the Saint-Chales River, Quebec, Canada. *Proceedings of the 39th IAHR World Congress*, Granada. <https://doi.org/10.3850/IAHR-39WC252171192022627>
- Elkurdy, M., Binns, A.D., Bonakdari, H., Gharabaghi, B. and McBean, E. (2022). Early detection of riverine flooding events using the group method of data handling for the Bow River, Alberta, Canada. *International Journal of River Basin Management*, 20(4), 533-544. <https://doi.org/10.1080/15715124.2021.1906261>
- EM-DAT. 2022 *Disasters in numbers: Climate in action*. <https://www.emdat.be/publications/> (accessed June 15, 2023).
- Environment Canada. *Canada's top ten weather stories for 2013*. <https://www.ec.gc.ca/meteo-weather/default.asp?lang=En&n=5BA5EAF1-1&offset=2&toc=show> (accessed June 15, 2014).
- Freiwan, M. and Cigizoglu, H.K. (2005). Prediction of total monthly rainfall in Jordan using feed forward backpropagation method. *Fresenius Environmental Bulletin*, 14(2), 142-151.
- Fronzi, D., Narang, G., Galdelli, A., Pepi, A., Mancini, A. and Tazioli, A. (2024). Towards groundwater-level prediction using Prophet fore-

- casting method by exploiting a high-resolution hydrogeological monitoring system. *Water*, 16(1), 152. <https://doi.org/10.3390/w16010152>
- Galdelli, A., Narang, G., Migliorelli, L., Izzo, A.D., Mancini, A. and Zingaretti, P. (2023). An AI-driven prototype for groundwater level prediction: Exploring the Gorgovivo Spring case study. *Proceedings of the International Conference on Image Analysis and Processing*, Udine, Italy. [http://dx.doi.org/10.1007/978-3-031-43153-1\\_35](http://dx.doi.org/10.1007/978-3-031-43153-1_35)
- Hamidouche, R., Aliouat, Z., Ari, A., and Gueroui, M. (2019). An efficient clustering strategy avoiding buffer overflow in IoT sensors: A bio-inspired based approach. *IEEE Access*, 7, 156733-156751. <https://doi.org/10.1109/ACCESS.2019.2943546>
- Hauswirth, S.M., van der Wiel, K., Bierkens, M.F., Beijl, V. and Wanders, N. (2023). Simulating hydrological extremes for different warming levels-combining large scale climate ensembles with local observation-based machine learning models. *Frontiers in Water*, 5, 1108108. <https://doi.org/10.3389/frwa.2023.1108108>
- Hsieh, W.W. (2023). Improving predictions by nonlinear regression models from outlying input data. *Journal of Environmental Informatics*, 41(2), 75-87. <https://doi.org/10.3808/jei.202300493>
- Ivakhnenko, A.G. (1968). The Group Method of Data Handling – A Rival of the Method of Stochastic Approximation. *Soviet Automatic Control*, 13(3), 43-55.
- Kharroubi, O., Blanpain, O., Masson, E., and Lallahem, S. (2016). Application du réseau des neurones artificiels à la prévision des débits horaires: Cas du bassin versant de l'Eure, France. *Hydrological Sciences Journal*, 61(3), 541-550. <https://doi.org/10.1080/02626667.2014.933225>
- Leandro, J., Chen, A.S., Djordjevi, S. and Savi, D.A. (2009). Comparison of 1D/1D and 1D/2D coupled (sewer/surface) hydraulic models for urban flood simulation. *Journal of Hydraulic Engineering*, 135(6), 495-504. [https://doi.org/10.1061/\(ASCE\)HY.1943-7900.0000037](https://doi.org/10.1061/(ASCE)HY.1943-7900.0000037)
- Lhomme, J., Bouvier, C., Mignot, E. and Paquier, A. (2006). One-dimensional GIS-based model compared to two-dimensional model in urban floods simulation. *Water Science & Technology*, 54(6-7), 83-91. <https://doi.org/10.2166/wst.2006.594>
- Machiwal, D. and Jha, M.K. (2012). Hydrologic time series analysis: Theory and practice. *Hydrologic Time Series Analysis: Theory and Practice*. Springer Netherlands, pp 85-94. <https://doi.org/10.1007/978-94-007-1861-6>
- Munji, C.A., Bele, M.Y., Nkwatoh, A.F., Idinoba, M.E., Somorin, O.A., and Sonwa, D.J. (2013). Vulnerability to coastal flooding and response strategies: The case of settlements in Cameroon mangrove forests. *Environmental Development*, 5(1), 54-72. <https://doi.org/10.1016/j.envdev.2012.10.002>
- Njoya, A.N., Ari, A.A.A., Nana Awa, M., Titouna, C., Labraoui, N., Effa, J.Y., Abdou W. and Gueroui, A. (2020). Hybrid wireless sensors deployment scheme with connectivity and coverage maintaining in wireless sensor networks. *Wireless Personal Communications*, 112, 1893-1917. <https://doi.org/10.1007/s11277-020-07132-5>
- Noakes, D.J., McLeod, A.I. and Hipel, K.W. (1985). Forecasting monthly river flow time series. *International Journal of Forecasting*, 1(2), 179-190. [https://doi.org/10.1016/0169-2070\(85\)90022-6](https://doi.org/10.1016/0169-2070(85)90022-6)
- Papacharalampous, G., Tyralis, H. and Koutsoyiannis, D. (2018). Predictability of monthly temperature and precipitation using automatic time series forecasting methods. *Acta Geophysica*, 66, 807-831. <https://doi.org/10.1007/s11600-018-0120-7>
- Papacharalampous, G.A. and Tyralis, H. (2018). Evaluation of random forests and Prophet for daily streamflow forecasting. *Advances in Geosciences*, 45, 201-208. <https://doi.org/10.5194/adgeo-45-201-2018>
- Pomeroy, J.W., Stewart, R.E. and Whitfield, P.H. (2016). The 2013 flood event in the South Saskatchewan and Elk River basins: Causes, assessment and damages. *Canadian Water Resources Journal*, 41(1), 105-117. <http://dx.doi.org/10.1080/07011784.2015.1089190>
- Public Safety Canada. Canadian Disaster Database. <https://open.canada.ca/data/en/dataset/1c3d15f9-9cfa-4010-8462-0d67e493d9b9> (accessed June 15, 2022).
- Riad, S., Mania, J., Bouchacou, L. and Najjar, Y. (2004). Rainfall-runoff model using an artificial neural network approach. *Mathematical and Computer Modelling*, 40, 839-846. <https://doi.org/10.1016/j.mcm.2004.10.012>
- Rood, S.B., Foster, S.G., Hillman, E.J., Luek, A. and Zanewich, K.P. (2016). Flood moderation: Declining peak flows along some Rocky Mountain rivers and the underlying mechanism. *Journal of Hydrology*, 536, 174-182. <http://dx.doi.org/10.1016/j.jhydrol.2016.02.043>
- Samsudin, R., Saad, P. and Shabri, A. (2011). River flow time series using least squares support vector machines. *Hydrology and Earth System Sciences*, 15(6), 1835-1852. <https://doi.org/10.5194/hess-15-1835-2011>
- Satour, N., Benyacoub, B., El Moçayd, N., Ennaimani, Z., Niazi, S., Kassou, N. and Kacimi, I. (2023). Machine Learning Enhances Flood Resilience Measurement in a Coastal Area-Case Study of Morocco. *Journal of Environmental Informatics*, 42(1), 53-64. <https://doi.org/10.3808/jei.202300497>
- Sehgal, V., Tiwari, M.K. and Chatterjee, C. (2014). Wavelet bootstrap multiple linear regression based hybrid modeling for daily river discharge forecasting. *Water Resources Management*, 28, 2793-2811. <https://doi.org/10.1007/s11269-014-0638-7>
- Slater, L.J., Arnal, L., Boucher, M.A., Chang, A.Y.Y., Moulds, S., Murphy, C., Nearing, G., Shalev, G., Shen, C., Speight, L., Villarini, G., Wilby, R.L., Wood, A. and Zappa, M. (2023). Hybrid forecasting: Blending climate predictions with AI models. *Hydrology and Earth System Sciences*, 27, 1865-1889. <https://doi.org/10.5194/hess-27-1865-2023>
- Suykens, J.A.K. and Vandewalle, J. (1999). Least squares support vector machine classifiers. *Neural Processing Letters*, 9, 293-300. <https://link.springer.com/article/10.1023/A:1018628609742>
- Taylor, S.J. and Letham, B. (2018). Forecasting at scale. *The American Statistician*, 72(1), 37-45. <https://doi.org/10.1080/00031305.2017.1380080>
- Tiwari, M.K. and Adamowski, J.F. (2017). An ensemble wavelet bootstrap machine learning approach to water demand forecasting: A case study in the city of Calgary, Canada. *Urban Water Journal*, 14, 185-201. <https://doi.org/10.1080/1573062X.2015.1084011>
- Van Wagner, C., Finney, M.A. and Heathcott, M. (2006). Historical fire cycles in the Canadian Rocky Mountain parks. *Forest Science*, 52(6), 704-717. <http://dx.doi.org/10.1093/forestscience/52.6.704>
- Vapnik, V. (1995). *The nature of statistical learning theory*. Springer New York, pp 181-216. <https://doi.org/10.1007/978-1-4757-3264-1>
- Veiga, V.B., Hassan, Q.K. and He, J. (2015). Development of flow forecasting models in the Bow River at Calgary, Alberta, Canada. *Water*, 7(1), 99-115. <https://doi.org/10.3390/w7010099>
- Walton, R., Binns, A., Bonakdari, H., Ebtehaj, I. and Gharabaghi, B. (2019). Estimating 2-year flood flows using the generalized structure of the Group Method of Data Handling. *Journal of Hydrology*, 575, 671-689. <https://doi.org/10.1016/j.jhydrol.2019.05.068>
- Wang, L., Xiao, T., Liu, S., Zhang, W., Yang, B. and Chen, L. (2023). Quantification of model uncertainty and variability for landslide displacement prediction based on Monte Carlo simulation. *Gondwana Research*, 123, 27-40. <https://doi.org/10.1016/j.gr.2023.03.006>
- Wang, Q. and Wang, S. (2020). Machine learning-based water level prediction in Lake Erie. *Water*, 12(10), 2654. <https://doi.org/10.3390/w12102654>
- Wang, W. (2006). *Stochasticity, nonlinearity and forecasting of stream-flow processes*. IOS Press: Amsterdam, pp 19-99. ISBN 978-1-58603-621-8
- Wang, W.C., Chau, K.W., Cheng, C.T. and Qiu, L. (2009). A comparison of performance of several artificial intelligence methods for forecasting monthly discharge time series. *Journal of Hydrology*, 3-

- 4, 294-306. <https://doi.org/10.1016/j.jhydrol.2009.06.019>
- Whitfield, P.H. and Pomeroy, J.W. (2016). Changes to flood peaks of a mountain river: Implications for analysis of the 2013 flood in the Upper Bow River, Canada. *Hydrological Process*, 30(25), 4657-4673. <https://doi.org/10.1002/hyp.10957>
- Xu, D.M., Wang, W.C., Chau, K.W., Cheng, C.T. and Chen, S.Y. (2013). Comparison of three global optimization algorithms for calibration of the Xinanjiang model parameters. *Journal of Hydroinformatics*, 15(1), 174-193. <https://doi.org/10.2166/hydro.2012.053>
- Yurekli, K., Kurunc, A. and Simsek, H. (2004). Prediction of daily maximum streamflow based on stochastic approaches. *Journal of Spatial Hydrology*, 4(2), 1-12.
- Zarinmehr, H., Tizro, A.T., Fryar, A.E., Pour, M.K. and Fasihi, R. (2022). Prediction of groundwater level variations based on gravity recovery and climate experiment (GRACE) satellite data and a time-series analysis: A case study in the Lake Urmia basin, Iran. *Environmental Earth Sciences*, 81, 180. <https://doi.org/10.1007/s12665-022-10296-x>
- Zhang, Z., Zhang, Q. and Singh, V.P. (2018). Univariate streamflow forecasting using commonly used data-driven models: Literature review and case study. *Hydrological Sciences Journal*, 63(7), 1091-1111. <https://doi.org/10.1080/02626667.2018.1469756>